2017

The effect of the chromoshadow domains of Hhp1, Hpl1, and Hpl2 on heterochromatin protein localization in Tetrahymena thermophila

Claire Bagnani
Scripps College

The effect of the chromoshadow domains of Hhp1, Hpl1, and Hpl2 on heterochromatin protein localization in *Tetrahymena thermophila*

A Thesis Presented
By Claire Bagnani

To the Keck Science Department
Of Claremont McKenna, Pitzer, and Scripps Colleges
In partial fulfillment of
The degree of Bachelor of Arts

Senior Thesis in Molecular Biology
December 4, 2016

Table of Contents

Abstract

In the nucleus, post-translational modifications on histone N-terminal tails can determine how local DNA is packaged. In one case, *T. thermophila* proteins Hhp1, Hpl1, and Hpl2, all related to the Heterochromatin Protein 1 (HP1) family, are associated with heterochromatin and thus gene silencing. They may do this by binding to trimethylated lysine 9 and lysine 27, located on the tail of histone H3. One distinct region of these proteins, the chromodomain (CD), may bind these marks, while another region, the chromoshadow domain (CSD) homodimerizes to interact with other proteins. This study explores what effect, if any, the CSD has on the CD's ability to localize to chromatin bodies marked by these post-translational modifications on the tail of H3. GFP tagged chromoshadow domain deficient Hhp1, Hpl1, and Hpl2 were overexpressed in *T. thermophila* cells and the localization of these proteins to chromatin bodies in the macronuclei during vegetative growth or developing macronuclei during conjugation was assessed using fluorescence microscopy. The retention of the trimethylated lysine 27 mark was also assessed in cells expressing CSD deficient Hhp1 using immunofluorescence microscopy. The results suggest that the chromoshadow domains of all proteins disrupt typical wild type localization patterns to different degrees. The CSD of Hpl2 seems to have more of an effect on localization than the CSD of Hhp1 and Hpl1.

Introduction

Epigenetics is the study of changes in gene function that are not due to changes in the gene sequence (Han and Garcia, 2013). Understanding the underlying mechanisms regarding epigenetics has implications for human health. Epigenetics may be key to understanding the extent of pathogen damage on humans, leading scientists to research drugs that target epigenetic function (Han and Garcia, 2013). In addition, there is research supporting the involvement of epigenetics in many human illnesses like cancer and autoimmune diseases and in processes like the diversification of cells (Han and Garcia, 2013; reviewed in Schwartzman and Tanay, 2015). Looking at single cells is the most direct way to investigate the role of epigenetics in development and differentiation because it avoids the need to categorize cell populations and eliminates the possibility of categorizing a group of cells as homogeneous and therefore epigenetically similar that actually contain vastly different chromatin dynamics (reviewed in Schwartzman and Tanay, 2015). Studying a single celled organism like *T. thermophila* would make investigating the relationships between histone modifications and gene expression easier.

Epigenetic mechanisms may lead to differential gene expression; the modulation of whether a gene product is made and the quantity of product. Gene expression could contribute to variation seen in human diseases like ovarian cancer and can be changed under certain circumstances like during exercise in humans (Laughlin et al., 2015; Villegas-Ruiz, 2016). This study seeks to uncover more information about mechanisms underlying the epigenetic packaging that includes condensing and decondensing the genome using a single cell model.

DNA Packaging in the Nucleus:

In order to be contained by the nucleus, DNA, must be compacted in a way that allows it to remain accessible (reviewed in Hergeth and Schneider, 2015). The first level of this DNA packaging involves proteins called histones (Luger et al., 1997). DNA wraps around a complex composed of two of each of the four core histones (H2A, H2B H3, and H4) forming nucleosomes, which make up chromatin (Luger et al., 1997). Nucleosomes are separated by short stretches of DNA, which resemble an arrangement similar to beads on a string (reviewed in Hergeth and Schneider, 2015). Linker histone H1 binds to the DNA between two nucleosomes (Robinson and Rhodes, 2006). This binding allows H1 to regulate the spacing of successive nucleosomes as well as the organization of nucleosome-nucleosome interaction, thereby stabilizing chromatin (Robinson and Rhodes, 2006).

Chromatin can be organized into heterochromatin or euchromatin (Figure 1). In contrast, heterochromatin is composed of tightly wound DNA, which, by limiting RNA polymerase accessibility, causes heterochromatin to be associated with transcriptional silencing (Huang et al., 1998). There are two types of heterochromatin, facultative and constitutive. Facultative heterochromatin (fHC) can oscillate between compact heterochromatin and less compact euchromatin-like conformations depending on spatial, temporal, and heritable genetic influences (reviewed in Trojer and Reinberg, 2007). Therefore, fHC can be packaged in a variety of condensed confirmations (reviewed in Trojer and Reinberg, 2007). Even though fHC is still considered transcriptionally silent, cytologically, it looks like constitutive heterochromatin or euchromatin (reviewed in Trojer and Reinberg, 2007). Unlike fHC, constitutive heterochromatin (cHC) remains

highly compact (reviewed in Grewal and Jia, 2007). It is typically located in centromeres and repetitive elements like transposons and maintains DNA stability and integrity by limiting transcriptional activation of transposons and recombination of repetitive elements (Jamieson et al., 2016; reviewed in Grewal and Jia, 2007; Wang et al., 2016). In contrast, transcriptionally active genes can be found in euchromatin, which contains more genes and is less condensed than heterochromatin (reviewed in Wang et al., 2016).

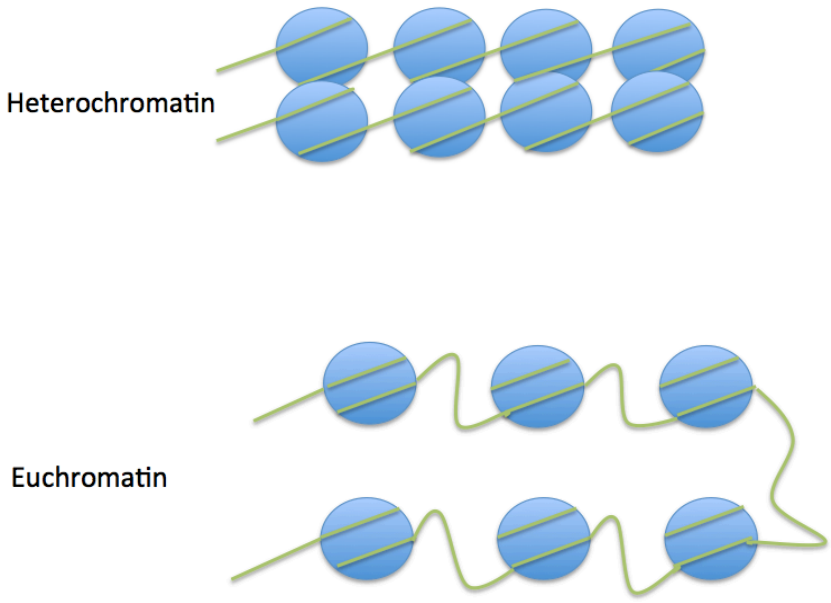

Figure 1. The two main forms of DNA packaging: heterochromatin and euchromatin (blue=nucleosomes, green=DNA).

Histone Modifications:

Whether chromatin is organized into euchromatin or heterochromatin is due in part to post-translational modifications on histone tails. Histone tails on either heterochromatin or euchromatin radiate out from the nucleosome and are more readily accessible to modification machinery than DNA (Jenuwein and Allis, 2001). Post-

translation chemical marks can be added to the residues on these tails and serve two general purposes. They can change the chromatin formation like lysine acetylation, which removes the negative charge from lysine (Shogren-Knaak, 2006). Or, post-translational modifications (PTMs) can recruit other proteins called 'readers' that bind to the PTMs and cause changes in downstream chromatin dynamics (reviewed in Rothbart and Strahl, 2015). PTMs modify the organization and function of chromatin by initiating transcription in a previously silent domain or silencing a normally active gene (Campos and Reinberg, 2009; Hayashi et al., 2009; reviewed in Kouzarides, 2007). Environmental cues modulate PTMs to regulate gene expression at the right time and place (Akai et al., 2010). The amalgamation of all histone modifications, which can work by themselves or in combination with other PTMs, translates into a code that can be used to understand gene dynamics at certain regions of chromatin (Jenuwein and Allis, 2001; reviewed in Rothbart and Strahl, 2015).

The tail of histone H3, of particular interest to this paper, can be post-translationally modified by acetylation, phosphorylation, and methylation. PTMs on histone H3 are best studied in organisms like yeast, mice, and humans or in general, but can be applied to *T. Thermophila.* In yeast, modifications H3K14 (lysine 14 on histone H3), H3K9, H3K18, H3K23, H3K27, and H3K36 can be acetylated using Gcn5 (Suka et al., 2001). This acetyltransferase commonly acetylates H3K27 on newly created histone H3 (Burgess et al., 2010). Other H3 lysine residues are associated with transcriptional activation when acetylated. This includes acetylated H3K56, which allows DNA to unravel from the histone core, permitting for protein accessibility and acetylated H3K64, which facilitates nucleosome stability and is associated with transcription in mice and

humans (reviewed in Bowman and Poirier, 2015; Di Cerbo et al., 2014). However, data suggest that acetylation function is dependent on the residue, there is no overarching rule regarding the role of every amino acid that is acetylated (Suganuma and Workman, 2011). Histone deacetylases oppose histone acetyltransferases and removes the acetyl groups from histones (Tauton et al., 1996).

Common phosphorylation sites on histone H3 are serine 10 and 28 and threonine 3 and 11 (reviewed in Banerjee and Chakravarti, 2011). Phosphorylation of H3 can occur during chromatin compaction in mitosis of mammalian cells (Hendzel et al., 1997). For example, serine 10, serine 28, and threonine 3 are all phosphorylated during mitosis (reviewed in Banerjee and Chakravarti, 2011; Di Croce and Shiekhatter, 2008; Hendzel et al., 1997). Also, threonine 11 phosphorylation may influence transcription (Di Croce and Shiekhatter, 2008). Additionally, histone phosphorylation can be involved in apoptosis and DNA repair (reviewed in Cheung et al., 2000). These H3 residues are phosphorylated by Ipl1/aurora kinase and dephosphorylated by Glc7/PP1 phosphatase in *S. cerevisae* and nematodes (reviewed in Hsu et al., 2000). Interestingly, in a case of histone modification cross talk, the phosphorylation of H3S10 by aurora B kinase could cause HP1, a reader of H3K9me3 to dissociate from that methyl mark (reviewed in Banerjee and Chakravarti, 2011; Fischle et al., 2005).

Histone H3 can be methylated on lysines 4, 9, 36, and 79 in yeast (reviewed in Law and Ciccaglione, 2015; Nakayama et al., 2001). Lysine 4 and 36 are commonly involved in euchromatin and transcriptional activation (reviewed in Wagner and Carpenter, 2014; Santos-Rosa et al., 2002). More specifically, methylated lysine 36 is involved in alternative splicing, DNA repair, and dosage compensation (reviewed in

Wagner and Carpenter, 2014). H3K9 methylation is associated with gene silencing in yeast and could repress tumors in humans (Nakayama et al., 2001; Yang et al., 2013). The methylation of lysine is also associated with transcriptional inactivation in another organism, *Tetrahymena thermophila*. H3K27me3 is prevalent in pockets of condensed chromatin in *T. thermophila* (Yale et al., 2016).

Histone methyltransferases and demethylases control the methylation status of histone residues (reviewed in Alam et al., 2015). These proteins modulate gene expression by either methylating (in the case of methyltransferases) or demethylating (in the case of demethylases) histones (reviewed in Law and Ciccaglione, 2015, reviewed in Alam et al., 2015). Dysregulation of lysine methylation can have drastic consequences. Lysine methylation that is not regulated properly can cause errors in meiosis and apoptosis in *S. cerevisiae* and humans and methylation at the incorrect site could lead to disease in humans (reviewed San-Segundo and Roeder, 2000; reviewed in Wagner and Carpenter, 2014; Walter et al, 2014).

Heterochromatin Proteins as Readers of Histone Modifications:

As mentioned above, PTMs can lead to changes in chromatin formation and dynamics by way of protein readers that bind to these modifications. The Heterochromatin protein 1 (HP1) family is a class of proteins that act as readers. These proteins bind di/trimethylated lysine 9 with conserved regions towards the amino terminus called chromodomains (Figure 2; Bannister et al., 2001; Lachner et al., 2001; Lomberk et al., 2006).

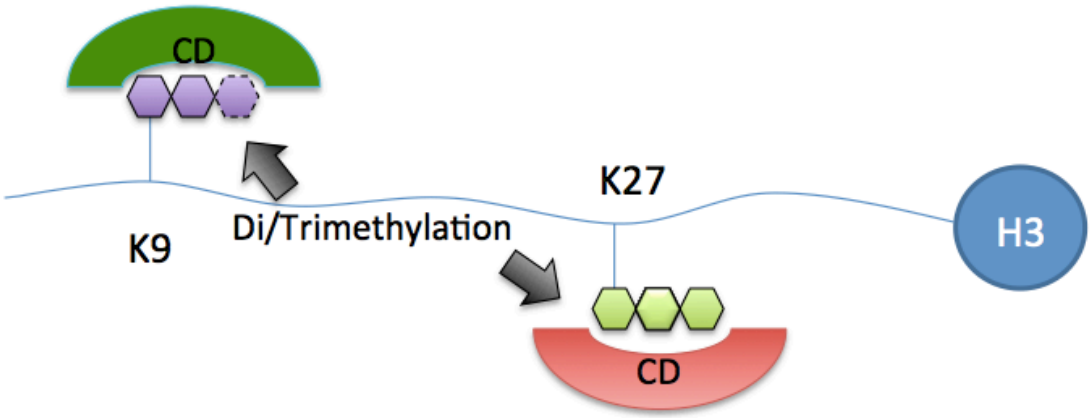

Figure 2. The chromodomain (CD) of HP1 family proteins recognizes and binds K27me3 (in the case of *T. thermophila*) and/or K9me2/3.

The first chromodomain-containing protein found was heterochromatin protein 1a (HP1a) in *D. melanogaster,* found to be a repressor of position-effect variegation, which occurs when euchromatin gets silenced when it is moved near heterochromatin (Lomberk et al., 2006). The chromodomain (CD) of HP1a interacts with dimethylated or trimethylated lysine 9 on the tail of H3, marks that are associated with heterochromatin and subsequent gene silencing (Eissenberg and Elgin, 2014; Lomberk et al., 2006). After binding to methylated lysine, HP1a recruits enzymes that facilitate chromatin compaction (Eissenberg and Elgin, 2014). Within HP1a's broader function of compacting chromatin, HP1a specifically promotes genome integrity and is involved with telomere capping and elongation (Eissenberg and Elgin, 2014). The creation of heterochromatin may be a remnant of a defense against transposable elements that could endanger the genome if not silenced (Eissenberg and Elgin, 2014).

HP1a as an Example of a Heterochromatin Protein:

The HP1a protein has two other distinct regions in addition to the chromodomain (Figure 3). The hinge or linker region connects the CD to the CSD and has the most variation across different heterochromatin proteins (Eissenberg and Elgin, 2014; Lomberk et al., 2006). More importantly, the hinge region can be phosphorylated by protein kinase A (Badugu et al., 2005). Phosphorylation of this region is associated with its ability to target heterochromatin and a reduction of the proteins ability to induce gene silencing (Badugu et al., 2005; Eissenberg et al., 1994; Zhao and Eissenberg, 1999). It is still unknown, however, the exact sites where the hinge region is phosphorylated in any organism (Badugu et al., 2005). Due to the widespread effects of modifications on the hinge region, it is considered to be the control center of the protein (Lomberk et al., 2006).

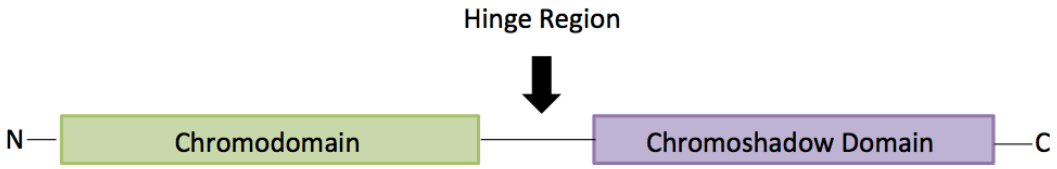

Figure 3. The three main regions of HP1a and all other members of the Heterochromatin Protein 1 family.

The chromoshadow domain is what distinguishes heterochromatin proteins from other chromodomain-containing proteins (Lomberk et al., 2006). One function of the CSD is regulation of histone modifications, which in turn regulate chromatin dynamics. For example, the CSD of HP1a binds a suppressor of a histone methyltransferase that

methylates H3K9 (Eissenberg and Elgin, 2014). The binding of the CSD of HP1a to dKDM4A a protein that demethylates H3K36, could be involved in regulating chromatin (Lin et al., 2008).

Additionally, the CSD of HP1a homodimerizes to prevent DNA from unwinding and thus stabilizes the nucleosome (Eissenberg and Elgin, 2014). There are two proposed conformations of homodimerization, one with the CDs homodimerizing and one without (Eissenberg and Elgin, 2014). Both confirmations keep the DNA inaccessible to transcription machinery (Eissenberg and Elgin, 2014). Dimerization creates a site for the docking of proteins containing the PxVxL motif that are involved in transcription (Thiru et al, 2004).

PxVxL proteins have not been studied in *T. thermophila,* so the interactions of PxVxL proteins with heterochromatin proteins in other organisms are used as a basis for understanding potential interactions of similar proteins in *T. thermophila*. The CSD of a mammalian heterochromatin protein, HP1α binds many nuclear proteins like KAP-1, CAF-1 p150, Sp110A and LBR through the PxVxL motif (Lechner et al., 2005). By binding these proteins, HP1α is involved in chromatin and sub-nuclear organization (Lechner et al., 2005). KAP-1 is a corepressor for proteins that contain the KRAB domain and causes transcriptional repression likely through its association with HP1 proteins (Lechner et al., 2000). CAF-1 (chromatin assembly factor 1) is involved in silencing retrotransposons (Hatanaka et al., 2015). Sp100 is an autoantigen that is targeted in acute promyelocytic leukemia (Seeler et al., 1998). Lamin B receptor (LBR) is located on the inner nuclear membrane and connects the inner membrane, lamina and chromatin of the nucleus (Herrmann and Zwerger, 2010). The association of the CSD of

mouse HPL1β with PxVxL containing proteins helps target HPL1β to heterochromatin (Thiru et al., 2004). In fact, the CSD of HP1α is necessary for the protein to localize to H3K9me3 (Mishima et al., 2013). All proteins in the Heterochromatin proteins 1 family by definition have a CD, a CSD, and a hinge region.

In humans, the CSD of HP1α, which is involved in H3 recognition and dimerization of the CSD, is required for H3 interaction (Richart et al., 2012). However, the effect of the CSD on the CD ability to bind chromatin modifications has not been explored in other HP1 family proteins in humans and in other organisms like the protist *Tetrahymena thermophila.* Studying the CSD in this organism would reveal the conservation of heterochromatin like proteins across organisms that have evolutionarily diverged many years ago. It would also aid in our understanding of the Heterochromatin Protein 1 family and of the effects of epigenetics at a single cell level.

Tetrahymena thermophila as a Model Organism for Gene Expression and Organization:

Tetrahymena thermophila, a single-celled ciliate protozoa, is an excellent organism to study the function of CSDs in more detail because it is commonly used to study gene organization and expression (Collins and Gorovsky, 2005). This is because these organisms have two different nuclei that function differently (Figure 4; Collins and Gorovsky, 2005). The macronucleus (MAC) is the somatic nucleus, which contains forty-five copies of transcriptionally active chromosomes (Collins and Gorovsky, 2005). The MAC is composed of euchromatin with patches of heterochromatin called chromatin bodies (Figure 4, green dots, Huang et al., 1998). This nucleus is the sole controller of the cell's phenotype during vegetative growth (Gorovsky, 1980). The micronucleus

(MIC), on the other hand, is the germline nucleus (Collins and Gorovsky, 2005). It is diploid and composed of constitutive heterochromatin, making it transcriptionally silent (Collins and Gorovsky, 2005). Using an organism that displays nuclear dimorphism like *T. thermophila* is ideal model for studying heterochromatin proteins, which impact chromatin organization. This is because the location and separation of each type of chromatin conformation is well known.

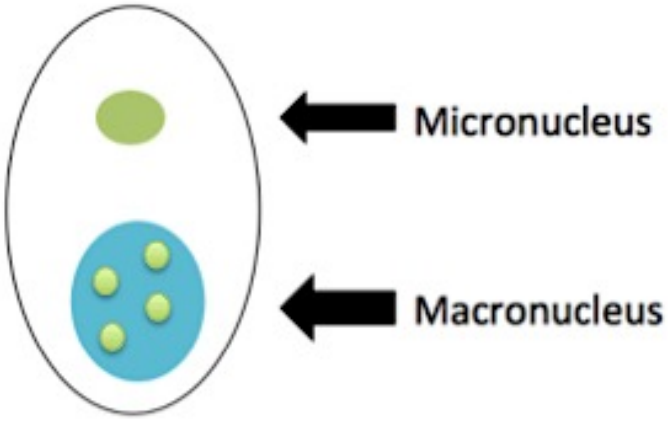

Figure 4. The two distinct nuclei of *Tetrahymena thermophila.*

During sexual conjugation, changes in chromatin conformation occur. The micronuclei of two organisms undergo meiosis and exchange their micronuclei, which differentiate into a new macronucleus (Collins and Gorovsky, 2005). During differentiation, the developing MAC undergoes DNA rearrangement where 34% of the micronuclear DNA is deleted (Yao et al., 2014). This occurs when internal elimination sequences (IES) mainly composed of repeated sequences are excised using an RNAi mechanism, condensed into heterochromatin and sent out of the nucleus (Figure 5; Xu et al., 2015; Liu et al., 2004). The resulting macronucleus destined sequences (MDs) are

fused together (Miao et al., 2009). The bundles of internal elimination sequences are seen in heterochromatin bodies that can be seen in the developing macronucleus in Figure 6. The IES's colocalize with H3K9me3, the histone mark that heterochromatin like proteins recognize and bind to facilitate the formation of heterochromatin (Liu et al., 2004). In fact, H3K9me3 is required for efficient IES processing (Liu et al., 2004).

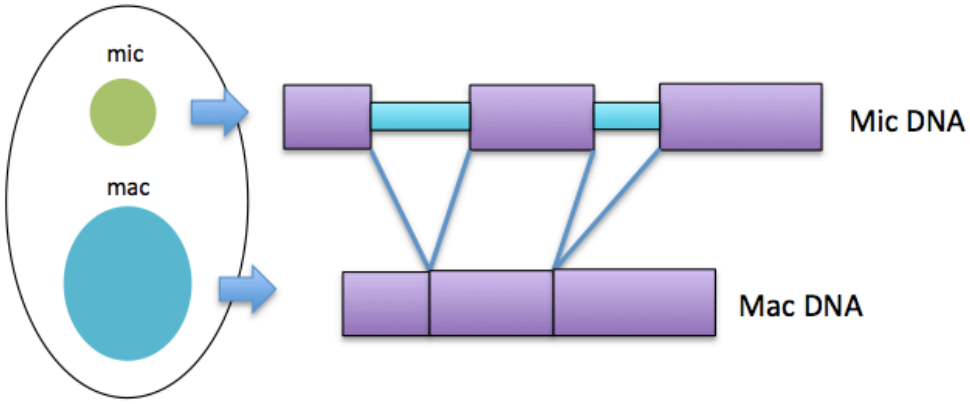

Figure 5. DNA rearrangement during sexual conjugation (blue bars=IES).

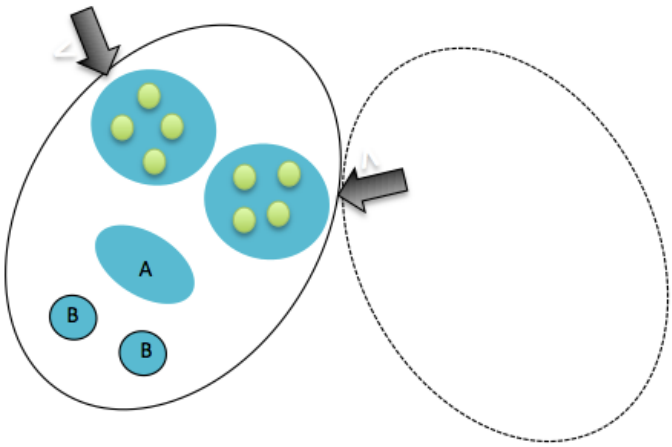

Figure 6. IES's as patches of heterochromatin (in green) in developing macronuclei (denoted by black arrows) during conjugation (A=old macronucleus, B=micronucleus)

Heterochromatin Proteins in *Tetrahymena thermophila:*

T. thermophila cells are especially useful because they have some chromosomes in common with humans and are genetically tractable, meaning that DNA can be transformed in *T. thermophila* (Collins and Gorovsky, 2005). They are unicellular so the effect of histone modification and gene expression can be studied more clearly. Additionally, Heterochromatin Protein 1 family homologs have been found in *T. thermophila*; of which, three of these, Hhp1, Hpl2, and Hpl1, will be investigated. It is not yet known how similar these proteins are to Heterochromatin Protein 1 family proteins in other organisms.

Hhp1p is one such protein found in the chromatin bodies in the MAC during vegetative growth (Figure 4; Huang et al., 1998). Due to evidence of its colocalization with the histone modification, it is speculated that Hhp1p binds to trimethylated H3K27, setting it apart from other proteins in the Heterochromatin Protein 1 family that only bind H3K9me2/3 (Yale et. al). However, despite this difference, Hhp1p is still associated with facultative heterochromatin due to its interaction with H3K27me3 mark (Jamieson et al., 2016; Yale et al., 2016). Similarly to HP1a, phosphorylation of a Cdc2/Cdk1 kinase site of the hinge region is necessary for colocalization of Hhp1 to this histone modification (Yale et al., 2016). Lastly, Hhp1p is involved in developmental changes that that occur during starvation (Miao et al., 2009). Hhp1 is associated with establishing and maintaining condensed chromatin as chromatin bodies that activate the expression of certain genes needed for starvation response that precedes mating (Huang et al., 1999).

Another HP-like protein, HPL2 is involved in mating. It is present in high numbers in the parental macronucleus 8-12 hours after conjugation and localizes to DNA

elimination structures that compose chromatin bodies formed in anlagen (the macronuclei that develop during conjugation) (Figure 6; Xu et al., 2015). Hpl2 (formerly known as Tcd1) is suspected to bind to H3K9me3 and H3K27me3, both of which are correlated to facultative heterochromatin (Jamieson et al., 2016; Peters et al., 2002; Xu et al., 2015). It is involved in heterochromatin formation, IES elimination using an RNAi like mechanism, and gene repair during MAC development (Xu et al., 2015).

The last heterochromatin protein this study is concerned with is Hpl1. Preliminary studies from Chalker lab show that Hpl localizes to IES elimination chromatin bodies. However, it is not yet known what histone modification Hpl1 binds as there is no literature on this protein currently. Due to its colocalization with Hpl2, for the purposes of this study, Hpl1 is suspected to bind H3K9me3 and H3K27me3.

Project Outline:

This study seeks to explore the purpose the chromoshadow domain in heterochromatin-like proteins play in heterochromatin formation. More specifically, this study focuses on whether the chromoshadow domain of Hhp1, Hpl1 and Hpl2 affects the ability of these proteins to localize to chromatin bodies marked with H3K9/27me3. Cells expressing the chromoshadow domain deficient proteins, Hhp1Δcsd, Hpl1Δcsd, and Hpl2Δcsd, were made by making mutant DNA constructs for each protein that eliminated the CSD leaving the CD and the hinge region (Figure 7). In order to investigate the function of the chromoshadow domain, localization of these mutant proteins in the macronucleus was used as an assay for the interaction between histone modifications and the CD and compared to the wild type (WT) proteins. Each protein was GFP tagged at

the N terminus so that localization of the protein could be seen by fluorescence microscopy.

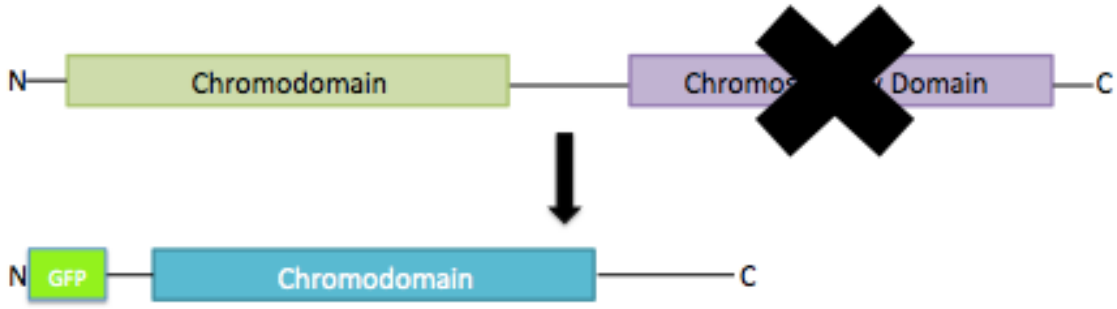

Figure 7. Chromoshadow domain exclusion mutation

Materials and Methods

Hhp1, Hpl1 and Hpl2 Related Cultures:

T. thermophila Cultures

Liquid cell cultures of B2, 428, Hhp1WT, and Hhp1Δcsd, Hpl1Δcsd, and Hpl2Δcsd, were grown in 100x sequestrene protease peptone (SPP) media (diluted from 10x SPP [10g yeast extract, 20g dextrose, 100g protease peptone in a 1 L solution]), with 0.2% iron chloride, 1X penicillin, streptomycine, and fungizone (PSF), and 0.01 mg/mL paromomycin. They were incubated at 30°C and shaken at 90 rpm. All cells were grown to mid-logarithmic phase ($1.8X10^5$ cells).

E. coli Cultures

Liquid cultures of E. coli were grown in a test tube with 5 mL Luria Broth (LB, 10 g tryptone, 5 g yeast extract, 10 g NaCl per liter, pH 7.5) and 50 μg/mL Kanamycin or 100 μg/mL Ampicilin. The cells were incubated on a 37°C shaker overnight. Cells were also grown on plates made of LB agar and the same concentrations of each drug.

Hhp1:

Live Cell Imaging

Tetrahymena cells transformed with Hhp1Δcsd by previous thesis student Alyssa Yoshino, were obtained and grown in SPP cultures overnight. Next, transcription within the cells was induced for 90 minutes by adding 1 mg/mL cadmium chloride to a final concentration of 2 μg/mL. The cells were then processed for live cell imaging by spinning 500 μL of the induced culture at 1,500 rcf for 2 minutes and then at the same speed for 1 minute. Next, 1 μL of 20 μg/mL of 4',6-Diamidino-2-phenylindole (DAPI)

was put on a glass slide. When the DAPI was dried, 5 μL of 3% methyl cellulose and 1 μL of cells were put on the slide and a Leica DM4000 B Led epifluorescence microscope was used to image the macronucleus of these cells. This process was also completed on Hhp1WT cells transformed with HHP1WT gene on the pIGF-GTW by Doug Chalker's lab.

Immunofluorescence

A liquid culture of Hhp1Δcsd and Hhp1WT cells were grown overnight and 5 mL of each culture was induced using the same cadmium chloride technique used for processing live cells. Next, the cells were centrifuged in separate conical vials at 250 rcf for 3 minutes and resuspended in pH 6.9 Pipes-Hepes-EGTA-$MgSO_4$ (PHEM) buffer [4.54 g 60 mM 1,4-Piperazinediethanesulfonic acid (PIPES), 1.5 g 25 mM 4-(2-hydroxyethyl)-1-piperazineethanesulfonic acid) (HEPES), 950 mg 10mM Ethylene glycol-bis(2-aminoethylether)-*N,N,N′,N′*-tetraacetic acid (EGTA), 100 mg 2mM $MgCl_2$, in a 250 mL deionized H_2O (dH_2O) solution].They were centrifuged again at 1500 rpm for two minutes. The pellet was fixed to a final concentration of $3X10^5$ cells/mL with 2% paraformaldehyde and triton (0.257% Triton x-100, 1mL 16% paraformaldehyde solution, in a 5 mL solution of PHEM). After an hour, the cells were centrifuged at 500 rcf for 5 minutes and washed with 500 μL PHEM buffer overnight.

Next, the cells were centrifuged at 500 rcf for 2 minutes and resuspended in about 1 mL of methanol. The cells for each strain were then dropped on coverslips . After the coverslips dried they were incubated for 1 hour in phosphate buffered saline (PBS) using Coplan jars. Two slips for each strain were placed facedown in a 100 μL puddle of a

1:500 solution of the primary antibody (Active Motif, mouse) in 1% bovine serum albumin in phosphate buffered saline with 0.1% tween (1% BSA in PBST). One cover slip for each strain, serving as the negative controls, was put in a 100 µL of 1% BSA in PBST. All coverslips were incubated at 4°C in a moist chamber overnight.

All slides were incubated in Coplan jars with PBST for 60 minutes, switching out the PBST every 10 minutes. They were placed facedown in 100 µL puddles of a 1:1500 solution of Active Motif goat α mouse rhodamine 2° antibody and incubated at 30°C for 30 minutes. Next, the slides were incubated n PBST for 60 minutes, replacing the PBST every 10 minutes. The slides were then put cell side down in 50 µL of 20 µg/mL DAPI and incubated at 25°C for five minutes. The slides were washed with dH_2O and then placed cell side down on slides with 5 µL of vectashield. Finally, the macronuclei of the cells were visualized using confocal microscopy.

Hpl1 and Hpl2

Primers

Forward and reverse primers were designed for HPL1Δcsd and HPL2Δcsd (Figure 8, Table 1). In both transcripts, the chromoshadow domain sequence was excluded. The expected product for HPL1Δcsd was 1,191 base pairs long and the product for HPL2Δcsd was 2,010 base pairs long. The primers were obtained from Integrated DNA Technologies.

Figure 8. Process of making mutant heterochromatin like protein transcripts by amplifying mutant primers (H=hinge region).

Table 1. Mutant heterochromatin like protein transcripts (bases complementary to each protein cDNA in bold)**.**

Primer	Sequence (5'-3')	Tm (°C)
HPL1Δcsd Forward	CACC**ATGGCTAAGATAAAATACGAAG**	58
HPL1Δcsd Reverse	TCA**ATTCGTTTTCCAGAACTGGA**	56
HPL2Δcsd Forward	CACC**ATGTTCACTGTAAAGCAACAG**	58
HPL2Δcsd Reverse	TCA**AAGATCTTGTAGAGTAGA**	56

Polymerase Chain Reaction (PCR) and Purification

To amplify HPL1 and HPL2, PCR was used using the Wizard® SV gel and PCR cleanup kit to manufacturer's instructions. Elution buffer (EB, 10 mM Tris-Cl pH 8.5) was added to the primers to suspend them to 100 µM. The primers were then diluted and 0.5 µM of the forward and reverse primers for both proteins were added to a solution containing 0.5 µg template Tetrahymena cDNA, 1.0 unit Phusion™ (taq) DNA polymerase, 1X Phusion™ High Fidelity buffer, 0.2 mM deoxynucleotide triphosphates

(dNTPs), and Milli Q water to a final volume of 50 µL. This solution was aliquoted into four tubes for each protein: one was a negative control that did not contain template DNA, and the other three were experimental with every ingredient. The PCR reaction involved 1 cycle at 98° C for 30 seconds, 30 cycles at 98° C for 10 seconds, 51-56° C for 20 seconds, and 72° C for 45 seconds, and another cycle at 72° C for 7 minutes. These were put in the MJ Research PTC-200 thermocycler and each experimental tube was put at a different temperature (based on the Tm of the primers) after they were heated to 98°C for 10 seconds to allow the primers to anneal to the DNA template. For HPL1Δcsd the tubes were placed at 52, 54, and 56°C. The HPL2 tubes were placed at 51, 53, and 55°C. The HPL1Δcsd negative control was heated at 52°C while the HPL2Δcsd negative control was subjected to 51°C.

Next, 10 µL of each sample was run at 500mA on a gel made of 1% agarose in Tris-acetate-EDTA (TAE, 40 mM Tris pH 7.6, 20 mM acetic acid, with 0.5 µL of ethidium bromide). The gel was visualized using a UV transiluminator to confirm that the DNA that was amplified using PCR was the right size. Next, the DNA was extract from the stock of PCR products by enough membrane binding solution so that there were equal volumes of PCR produce and membrane binding solution (40 µL). The solution was incubated at room temperature for 1 minute and centrifuged at 16 rcf. 700 µL of membrane wash solution was added and the samples were centrifuged at 12 rcf for 1 minute. Next, the samples were centrifuged again after washing with 500 µL of membrane wash solution. After letting the ethanol evaporate from the tubes, 30 µL of milliQ water was added, the tubes were incubated at room temperature for 1 minute and centrifuged again. The DNA was then quantified using a Thermo scientific NanoDrop™

2000 Spectrophotometer. The HPL1 DNA was concentrated at 37 ng/μL and the HPL2 DNA was concentrated at 68 ng/μL.

Cloning Truncated Proteins onto p-ENTR™ Vector

The HPL1 and HPL2 were cloned onto a pENTR™/TOPO® vector that included kanamycin resistance using chemically competent *E. coli*. Enough DNA was transferred to another tube to make 15 ng/μL of DNA in 10 μL. 15n ng of this dilute DNA for both HPL1 and HPL2 was added to 3 μL of miliQ water, 1 μL of a salt solution, and 1 μL of the TOPO vector as per manufacturer's instructions. The two tubes (one for each mutant) were centrifuged for 1 minute and incubated at room temperature for 30 minutes. 2 μL of the solution was added to chemically competent *E. coli* and incubated on ice for 15 minutes. Next, the tubes were heat shocked at 42°C for 30 seconds. Next, 250 μL of Super Optimal broth with Catabolite repression (SOC) medium [10 g bactotryptone, 2.5 g yeast extract, 0.29 g NaCl, 0.093 g KCl, 1.02 g $MgCl_2$, 1.23 g $MgSO_4$, 1.8 g glucose per 500 mL] was added to the tubes and they were incubated on a horizontal shaker at 200 rpm at 37°C for 1 hour. Then, two aliquots of the cells were plated on two kanamycin Luria broth plates for each mutant. The first aliquot was 200 μL and the second aliquot was the remainder of the tube. After growing overnight at 37°C, the cells were transferred into four LB + kanamycin liquid *E. coli* cultures for each protein using bacteria from a single colony. The liquid cultures were grown up at 37°C overnight.

Plasmid Preparation and Digestion

The plasmids were extracted from the liquid cultures using the Qiagen QIAprep spin miniprep kit. Two aliquots of 1.5 mL of the liquid cultures were centrifuged for 1 minute at 16,100 rcf and resuspended in 250 µL of buffer P1. Next, 250 µL of buffer P2 and 350 µL of buffer N3 were added and the tubes were inverted 6 times before they were centrifuged at 15,700 rcf for 10 minutes. The supernatant was extracted and centrifuged at 15,700 rcf for 1 minute. Next, 750 µL of buffer PE was added and centrifuged at 15,700 rcf for 1 minute twice. 50 µL of EB buffer was added and the tubes were incubated for 1 minute and centrifuged for 1 minute.

To digest the plasmids, 5 µL of plasmid from the plasmid prep were added to 2 µL of 10X digestion buffer, 12.5 µL milliQ water, and 0.5 µL of Not I enzyme. The tubes were put in a 37°C water bath for two hours. To confirm that the plasmids were successfully cloned, 20 µL of the digested plasmid were run on a 1% agarose gel and visualized using an UV transiluminator using the same procedure as was used after the PCR. To confirm that the correct plasmids were cloned, samples of HPL1Δcsd and HPL2Δcsd were sent to Integrated DNA Technologies to be sequenced.

Recombination onto pIGF-GTW Vector

HPL1Δcsd and HPL2Δcsd were transferred onto the pIGF-GTW vector, which contains a GFP tag on the 5' end (N terminus of resulting protein) and an ampicillin and paromomycin resistance gene on 3' gene (Figure 9). First, 50 ng of the pENTR^{TM} clone from the above plasmid prep was added to 4 ng pIGF-GTW destination vector and H_2O

to a volume of 4 µL. Next, 1 µL of LR clonase II enzyme was added and the tubes were incubated at room temperature overnight.

Next, the recombined plasmid was transformed into *E. coli* using electroporation. 1 µL of the recombination reaction was added to 50 µL of electrocompetent *E. coli* and the cells were pulsed with an electroporator at 1650 V, 200 Ω, and 25 µF. After, 500 µL of SOC medium was added and the cells were incubated on a shaker at 250 rpm at 37°C for one hour. The cells were plated on 100 µg/mL ampicillin Luria broth plates using two aliquots of 200 µL and 50 µL and incubated at 37°C overnight. Overnight liquid cultures with ampicillin were made using a single colony from the plates.

Figure 9. Recombination of Hpl1Δcsd and Hpl2Δcsd onto pIGF-GTW vector (Red=cell death gene, dark green=Hpl1/Hpl2 CD, light green=GFP gene, white=hinge region).

Plasmid Preparation and Digestion

To extract the plasmids, using the liquid cultures, 1.4 mL was centrifuged at 16,100 rpm for 1 minute. The cells were resuspended in 350 µL of sucrose lysis buffer (8% sucrose, 0.5% Triton X-100, 50mM EDTA and 100mMtris pH 8.0) and heated at 99°C for 4 minutes using a heat block. Next, the cells were centrifuged at 13,250 rcf for 15 minutes and the pellets were removed using a toothpick. 40 µL of 3 M NaOAC and 220 µL of isopropanol were added to the supernatant and it was incubated at room temperature for 5 minutes then centrifuged for 10 minutes. Next, the solutions were washed with 500 µL of 70% ethanol and centrifuged for 2 minutes. After drying, the pellets were resuspended in 50 µL of EB buffer.

To digest the plasmids, 5 µL of the plasmids from the last procedure were added to 2 µL of Cutsmart® buffer, 0.5 µL of Bam HI High Fidelity® enzyme and 12.5 µL milliQ water. The tubes were incubated in a 37°C water bath for two hours. 20 µL of the digested plasmid were run on a 1% agarose gel and visualized using an UV transiluminator using the same procedure used to confirm that the DNA construct was cloned successful.

Transformation

Plasmid Purification with HPL1 and HPL 2 mutants: Liquid cultures were made from ampicillin plates using the same procedure used after the recombination. Plasmids were purified using the QIAprep® Spin Miniprep Kit by Qiagen.

Preparing Tetrahymena cultures: Two cultures, B2 and 428 were used to inoculate 20 mL of Luria broth and 20 µL of ampicillin and incubated at 25°C overnight.

Next, the cells were starved by spinning them at 866 rcf for 3 minutes at 25°C. 30 mL of 10 mM Tris was added and the cells were centrifuged again. After this, 40 mL of Tris was added and each tube was poured into two 150 X 15 mm plates, put in a moist chamber to be incubated overnight. 13 hours later, the two plates were mated by mixing the two cultures together. 8 hours after the Tetrahymena was mated, the cells were staged to using epifluorescence microscopy to insure that cells were at the proper stage of conjugation with developing macronuclei.

Transformation: 1.5 hours after the cells were staged, 40 mL of the cells were centrifuged at 946 rpm for 5 minutes at room temperature and resuspended in 25 mL of 10 mM HEPES. After incubated at room temperature for 5 minutes they were centrifuged again and 200 μL of HEPES was added and the cells were electroporated at 225 V, 25Ω, and 175 μF. They were washed out with media (containing 100X SPP, with 0.2% iron chloride, 1X penicillin, streptomycine, and fungizone (PSF), and 0.01 mg/mL paromomycin and immediately transferred into a flask with the rest of the medium. After transformation was complete, the cultures were incubated at 25°C.

Live Cell Imaging

Cultures of B2, 428, Hpl1Δcsd, and Hpl2Δcsd were grown, starved, and mated using the same method used to prepare *T. thermophila* for transformation. Hpl1Δcsd and Hpl2Δcsd were each individually mated with B2 and 428 to determine which mating type the mutant strains would mate with. Both mutated cultures mated best with B2. After, transcription within the cells was induced for 90 minutes by adding 1mg/mL cadmium chloride to a final concentration of 2 μg/mL. The cells were then processed for live cell

imaging by spinning 500 µL of the induced culture at 1,500 rcf for 2 minutes and then at the same speed for 1 minute. Next, 1 µL of 20 µg/mL of 4',6-Diamidino-2-phenylindole (DAPI) was put on a glass slide. When the DAPI was dried, 5 µL of 3% methyl cellulose and 1 µL of cells were put on the slide and a Leica DM4000 B Led epifluorescence microscope was used to image the macronucleus of these cells. This process was also completed on Hhp1 Wild Type (WT) cells.

Results

The effect of the CSD of Hhp1, Hpl1 and Hpl2 on the localization of these proteins within the macronucleus was assessed by inducing the overexpression of GFP tagged truncated proteins that did not contain the chromoshadow domain and visualizing the expression pattern.

Properties of pENTR and pIGF-GTW Vector to Ensure Proper Cloning, Recombination, and Inducible Expression in *T. thermophila*

In order to visualize the localization of Hhp1Δcsd, Hpl1Δcsd, and Hpl2Δcsd (the mutant proteins), a vector containing the corresponding mutant genes must be transformed into *T. thermophila*. This vector, the pIGF-GTW vector, was also used to GFP-tagged the mutant genes so their expression could be seen using fluorescence microscopy. This process was already done by Alyssa Yoshino for the HHP1Δcsd construct. To achieve this process for the HPL1Δcsd and HPL2Δcsd, these constructs were cloned onto a pENTR™/TOPO® vector and transformed in *E. coli*. The pENTR™/TOPO® vector contained a kanamycin resistance gene so that all other cells that were not cloned with this vector would die when exposed to kanamycin (Figure 10).

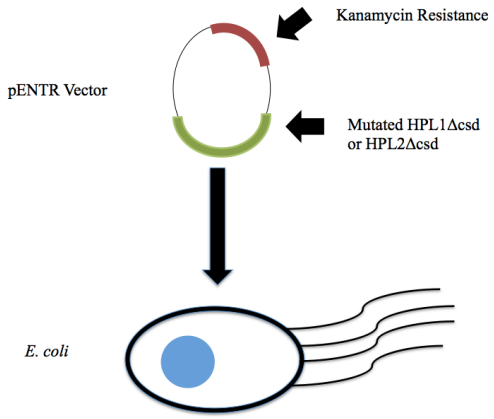

Figure 10. Schematic of the pENTR vector that was transformed into *E. coli*.

In order to transform the vector containing these genes into *T. thermophila* to induce overexpression, the vector had to be recombined onto the pIGF-GTW vector in *E. coli* that could be uptaked by the ciliates and to achieve GFP fusion. Properties of both vectors ensure that all of the products of the recombination were pIGF-GTW vectors with the truncated gene. The pIGF-GTW vector contains a gene that causes cell death in the location that gets swapped for the mutated genes. This gene induces cell death in all *E. coli* that contain the pIGF-GTW vectors that did not recombine with Hhp1Δcsd, Hpl1Δcsd, or Hpl2Δcsd. The ampicillin resistance gene on the pIGF-GTW vector prevents the survival of *E. coli* containing pENTR™/TOPO® vectors that still contain the Hhp1Δcsd, Hpl1Δcsd, or the Hpl2Δcsd gene. The pENTR™/TOPO® vector only contains a kanamycin resistance gene, so when the *E. coli* are exposed to ampicillin after recombination, the cells contain the pENTR™/TOPO® vector that failed to recombine would die (Figure 11).

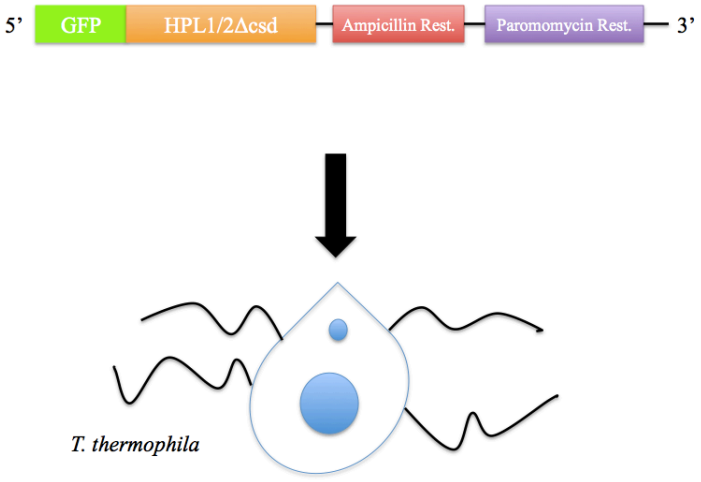

Figure 11. Schematic of pIGF-GTW vector (top, depicted as linear instead of circular) and the transformation of this vector into *T. thermophila.*

After transformation of the pIGF-GTW vector in Tetrahymena, expression of the mutant proteins was stimulated using the metallothionein (MTT) promoter. This promoter is found on the pIGF-GTW vector and is metal inducible (Boldrin et al., 2006). Cadmium chloride, a metal used in this lab, binds to activators that eventually led to the binding of RNA polymerase to the promoter and the initiation of transcription. The MTT promoter is naturally found in *T. thermophila*. Therefore, the activators and other factors that interact with cadmium chloride and other metals are present. Two hours after being exposed to cadmium chloride, the mutant proteins are expressed.

Confirmation that pENTR Vector Cloning was Successful

Both the HPL1Δcsd and HPL2Δcsd constructs were amplified without alteration as confirmed by sequencing and a 1% agarose gel (data not shown). To confirm that the constructs had been successfully cloned onto a 2,580 bp pENTR vector, gel electrophoresis using a restriction enzyme (NotI) digest was used (Figure 12). The expected DNA length for the pENTR vector containing HPL1Δcsd was 3771 bp and for HPL2Δcsd was 4590 bp. Lane 5 contained DNA 5000 bp and lane 6 contained DNA at 6000 bp. Running the gel for a longer period of time may result in a better resolution of the digest product. However, sequencing confirmed that mutagenesis was successful and the constructs were successfully cloned on the pENTR vector. Therefore, the reactions in lane 5 and 6 were used in the recombination experiment.

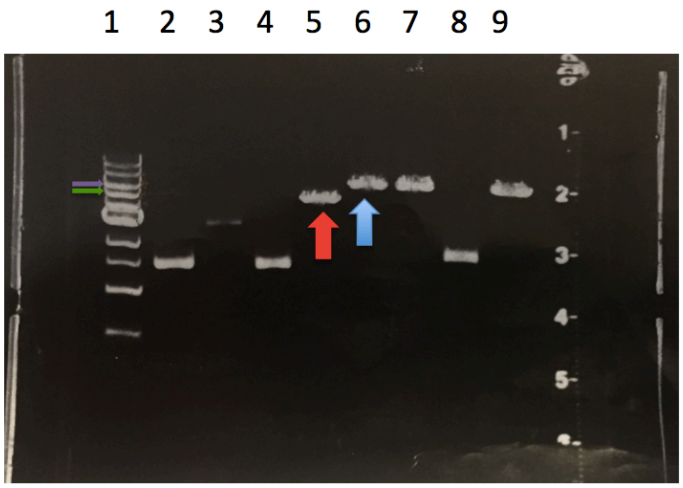

Figure 12. NotI digest of cloned HPL1ΔCSD and HPL2ΔCSD onto a pENTR vector using electrophoresis on a 1% agarose gel. Lane 2-5 contained cloning reactions with the HPL1Δcsd constructs while lane 6-9 contained cloning reactions with HPL2Δcsd. Purple arrow=6000 bp ladder band, green arrow=5000 bp ladder band, red arrow=HPL1Δcsd construct used for further experiments, blue arrow=HPL2Δcsd construct used for further experiments.

Confirmation of Successful Recombination of Constructs from pENTR Vector to pIGF-GTW Vector

To confirm that the constructs had been successfully recombined onto a 18145 bp pIGF-GTW vector, gel electrophoresis using a BamHI digest was used (Figure 13). The expected bands for HPL1Δcsd on the pIGF-GTW vector were 11268 bp, 3423 bp (the size of the construct plus 2232 bp), 2155 bp, and 424 bp. Lane 2 contained these band lengths. The expected bands for HPL2Δcsd on the pIGF-GTW vector were 11268 bp, 4242 bp (the size of the construct plus 2232 bp), 2155 bp, and 424 bp. Lane 7 contained these band lengths. This confirms that the reactions in lane 2 and lane 7 contained HPL1Δcsd and HPL2Δcsd successfully recombined on the pIGF-GTW vector. These reactions in lane 2 and lane 7 were then transformed into *T. thermophila.*

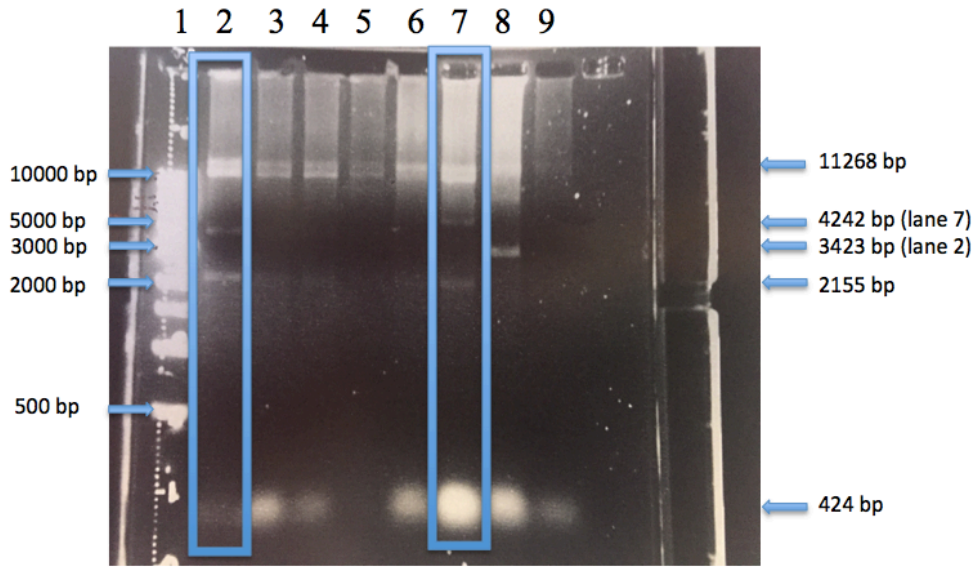

Figure 13. BamHI digest of recombined HPL1ΔCSD and HPL2ΔCSD on a pIGF-GTW vector using electrophoresis on a 1% agarose gel. Lane 1 contained a 1kb ladder while lane 2-5 contained recombination reactions with the HPL1Δcsd constructs and lane 6-9 contained recombination reactions with HPL2Δcsd. Lane 2 contained a successful HPL1Δcsd reaction and Lane 7 contained a successful HPL2Δcsd reaction.

Differential Localization Patterns of Hhp1Δcsd and Hhp1WT Within the Macronucleus

To determine if Hhp1Δcsd and Hhp1WT localize to the macronucleus as expected and if there is a difference in the localization pattern of Hhp1Δcsd and Hhp1WT within the macronucleus, *T. thermophila* cells transformed with pIGF-GTW vectors containing GFP-tagged HHP1Δcsd and HHP1WT were visualized using epifluorescence microscopy (Figure 14). Microscopy was done on *T. thermophila* in vegetative growth because Hhp1 is normally expressed during this stage. Hhp1WT and Hhp1Δcsd both localized to the macronucleus and their localization patterns were different.

The macronuclei of Hhp1WT cells contained punctate foci previously demonstrated to be chromatin bodies spread uniformly throughout the macronucleus (Figure 14C, arrow, Yale et al., 2016). This localization pattern is expected for Hhp1WT

because Hhp1 localizes to the chromatin bodies in the macronucleus (Huang et al., 1998). Conversely, the aggregates seen in around 70% of Hhp1Δcsd cells were fainter and less distinct indicating delocalization to chromatin bodies (Figure 14D, arrow). These data could suggest that the CSD of Hhp1 is needed for proper localization in the macronucleus. However, a possibility accounting for this difference in localization pattern is that the prevalence of histone modifications (presumably H3K27me3) is decreased in Hhp1Δcsd cells.

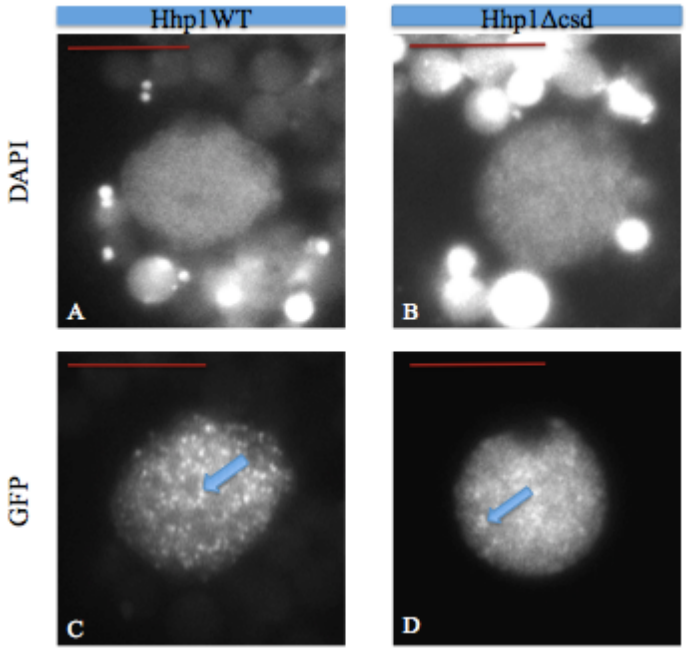

Figure 14. Epifluorescence microscopy of *T. thermophila* macronuclei during vegetative growth, stained with DAPI to detect DNA (A and B) and GFP tagged Hhp1WT and Hhp1Δcsd (C and D). Scale bars: 10 μm (A and C) and 16 μm (B and D). Arrows=aggregates of interest.

H3K27me3 Marks May be Preserved in Cells Expressing Hhp1Δcsd

To confirm that the differences seen in Hhp1Δcsd localization pattern were due to the inability of chromodomain to localize to H3K27me3 and not due to the absence of H3K27me3, the distribution of this histone mark was observed using immunofluorescence with rhodamine as the secondary antibody (Figure 15). Negative controls of cells in 1% BSA in PBST (the solvent used for the primary and secondary antibody) were made for Hhp1WT and Hhp1Δcsd. However, there were not enough cells to visualize.

The localization of the majority of the rhodamine stain to the macronucleus suggest that H3K27me3 is still present in the macronucleus of cells expressing Hhp1Δcsd. However, because there is a lot of background in the rhodamine stain of Hhp1Δcsd and Hhp1WT and punctate foci within the macronucleus are not visible, this data is inconclusive. While it seems like the H3K27me3 is still retained in the macronuclei of cells expressing Hhp1Δcsd, the methyl marks may be diffuse, which would suggest that it is the dispersion of H3K27me3 that is responsible for the localization pattern of Hhp1Δcsd in Figure 14. Furthermore, there were only three total cells that could be visualized, which calls for replication of this procedure to be more certain of this pattern.

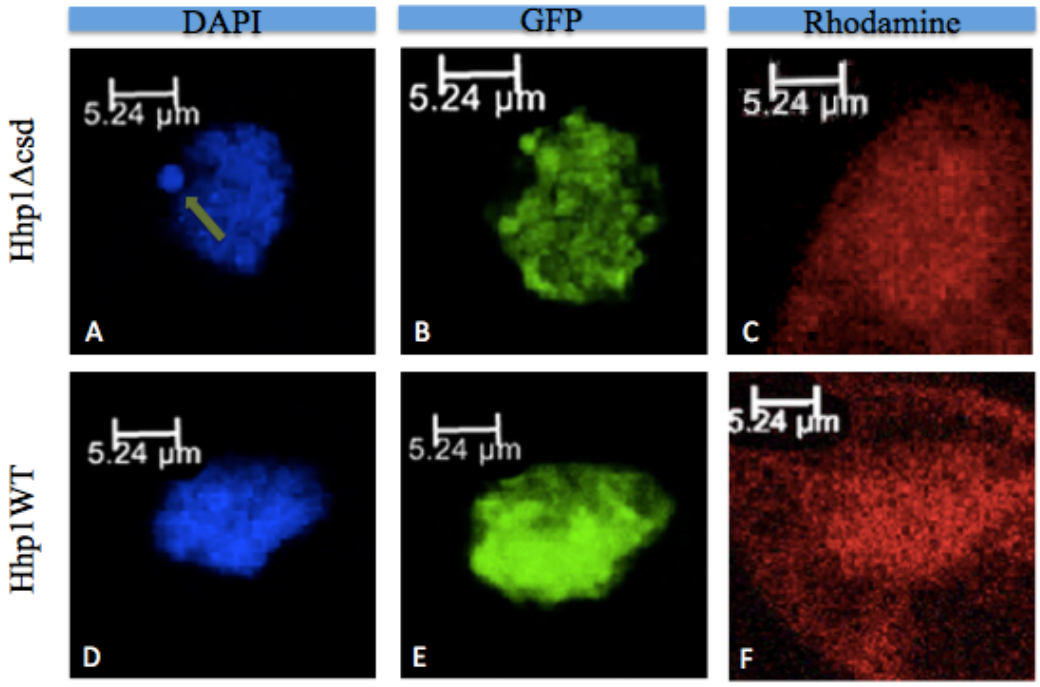

Figure 15. Confocal images of the macronuclei of growing cells expressing Hhp1Δcsd (A-C) and Hhp1WT (D-F). Hhp1WT and Hhp1Δcsd are tagged with GFP (green). The cells are additionally stained with DAPI (blue) to detect nuclei and rhodamine (red) to mark H3K27me3. Arrow=MIC.

Hpl1Δcsd Localization Forms Small Aggregates and is Expressed During Early Macronuclear Development and Vegetative Growth

To determine when another truncated protein, Hpl1Δcsd is expressed during macronuclear development and if its localization pattern during late macronuclear development differs compared to Hpl1WT, conjugated cells expressing Hplcsd were visualized using epifluorescence microscopy (Figure 16) and the localization of Hpl1Δcsd during late macronuclear development was compared to that of Hpl1WT (Figure 17). The expression pattern of these two species were compared during late macronuclear development because peak expression of Hpl1WT is observed during this stage (data not shown).

Hpl1Δcsd was expressed during early macronuclear and late macronuclear development (Figure 16 E, F). This suggest that the CSD of Hpl1 does not effect the timing of Hpl1 expression. This is because Hpl1Δcsd is normally expressed during early macronuclear development and reaches peak expression during late macronuclear development [data by Doug Chalker not shown]. Hpl1Δcsd expression was also induced during vegetative growth (Figure 16, D) when Hpl1 is not normally expressed to see if Hpl1Δcsd behaves like Hpl1WT. In both species, Hpl1Δcsd and Hpl1WT localize outside the macronucleus [data not shown for Hpl1WT localization]. This is unexpected considering the localization of both proteins to the developing macronucleus during conjugation but may be explained by the absence of H3K9 trimethylation in macronuclei during vegetative growth.

In around 60% of cells expressing Hpl1Δcsd, localization of this protein formed aggregates that were smaller than the punctate foci seen in Hpl1WT, that have been previously demonstrated to be chromatin bodies (Figure 17). This suggest that the CSD of Hpl1 may effect the size of the foci but doesn't seem to effect retention of some aggregate formation.

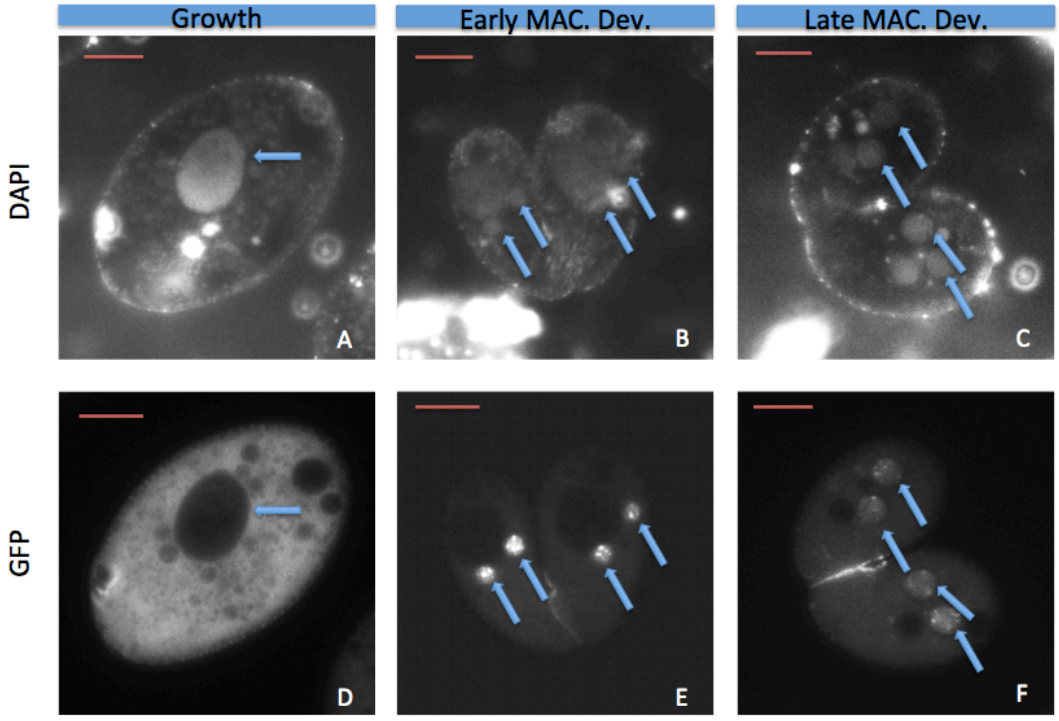

Figure 16. Epiflourescence microscopy showing the localization of Hpl1Δcsd during vegetative growth (A and D), early macronuclear development (~6 hours after conjugation, B and E), and late macronuclear development (~9 hours after conjugation, C and F) stained with DAPI to detect DNA and GFP tagged Hplcsd. Arrows point to the macronucleus (A and D) and anlagen (B,C,E,F) Scale bars:16 µm.

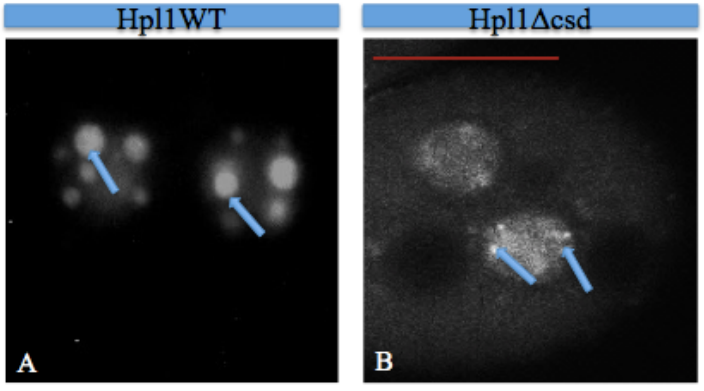

Image by Doug Chalker

Figure 17. Epifluorescence microscopy of mCherry-tagged Hpl1WT (A) and GFP-tagged Hpl1Δcsd (B) in anlagen (~9 hours after conjugation.) Arrows=aggregates of interest. Scale bar: 16 µm.

Lack of Aggregates in Hpl2Δcsd Localization Pattern and Expression of Hpl2Δcsd During Vegetative Growth

Hpl2 was the last protein to be investigated. To determine if the localization of Hpl2Δcsd during late macronuclear development differs compared to Hpl2WT, conjugated cells expressing Hpl2Δcsd were visualized using epifluorescence microscopy and compared to the localization of Hpl2WT (Figure 18). Similarly to the Hpl1Δcsd and Hpl1WT, cells during late macronuclear development (~9 hours after conjugation) were imaged because the expression pattern of Hpl1WT is highest during that time [data by Doug Chalker not shown].

The developing macronuclei of cells expressing Hpl2WT contain foci assumed to be chromatin bodies (Figure 18, A). However, in around 60% of conjugating cells expressing Hpl2Δcsd, the localization of this protein in the developing macronuclei is uniform and lacks chromatin bodies (Figure 18, B). The differences in the localization of Hpl2Δcsd and Hpl2WT may indicate that the chromoshadow domain is necessary for the localization of this protein to chromatin bodies.

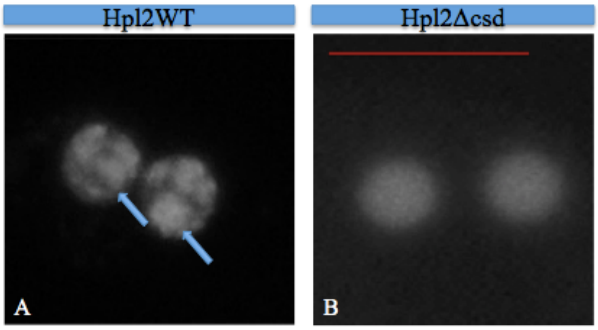

Figure 18. Epifluorescence microscopy of mCherry-tagged Hpl2WT (A) and GFP-tagged Hpl2Δcsd (B) in developing MACs (~9 hours after conjugation.) Arrows=aggregates of interest. Scale bar:16 μm.

The expression of Hpl2Δcsd was also forced during vegetative growth (when Hpl2 is not normally expressed) and compared to the expression during late macronuclear development (Figure 19). Hpl2Δcsd localizes to the macronucleus or anlagen during vegetative growth and late macronuclear development (Figure 19, B,C). Additionally, in both Hpl2Δcsd and Hpl2WT [data not shown] localize to the macronucleus. This may indicate that the lack of trimethylation on H3K9 does not prevent Hpl2WT and Hpl2Δcsd from targeting H3K27me3 in the macronucleus.

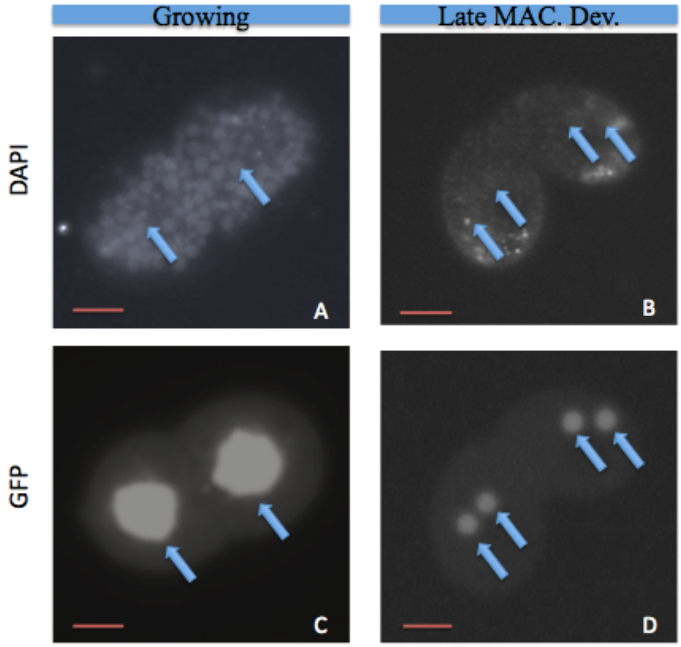

Figure 19. Localization of Hpl2Δcsd during vegetative growth of a cell going through asexual division (A and C) and late macronuclear development (~9 hours after conjugation, B and D) stained with DAPI to detect DNA and GFP tagged Hpl2Δcsd. Arrows point to the macronuclei (A, C) and developing macronuclei (B, D). A and B show *T. thermophila's* normal processing of DAPI using food vacuoles. Scale bars:16 μm.

Discussion

Epigenetic regulation of gene expression through compaction into heterochromatin involves accuracy in the timing a location of certain factors (Yale et al., 2016). Proteins in the Heterochromatin protein family are one such factor. This study investigated the effect of the chromoshadow domains of Hhp1, Hpl1, Hpl2 on the proteins ability to localize to chromatin bodies, which may be influenced by the chromodomains' potential interaction H3K27me3 and/or H3K9me3. It is one of the first studies to analyze the chromoshadow domain of Hpl2 and the first study on Hpl1.

Implication of Differences in Effect of CSD on Localization Within the Macronucleus

The results of this study suggest that the CSD of all proteins studied (Hhp1, Hpl1, and Hpl2) seem to effect localization of the protein to chromatin bodies in the macronucleus. The lack of any aggregate formation in Hpl2Δcsd anlagen compared to the less distinct foci in Hhp1Δcsd and the smaller foci in Hpl1Δcsd macronuclei suggest that the CSD of Hpl2Δcsd has more of an effect on localization to chromatin bodies than Hhp1 and Hpl1 (Figure 20). The differences in localization could be due to the CSD's effect on the CDs potential binding to H3K27me3 and/or H3K9me3. The preliminary mechanism shown in Figure 20 assumes that Hhp1, Hpl1 and Hpl2 bind these methyl marks even though this has only been suspected and not established. Also, to confirm that the lack of localization of Hpl2Δcsd to chromatin bodies is due to the lack of CSD and not the absence of H3K27me3 or H3K9me3, immunofluorescence microscopy with anti-H3K27me3 and anti-H3K9me3 should be done in a similar manner to the immunofluorescence microscopy of Hhp1Δcsd. This should also be done on Hpl1Δcsd.

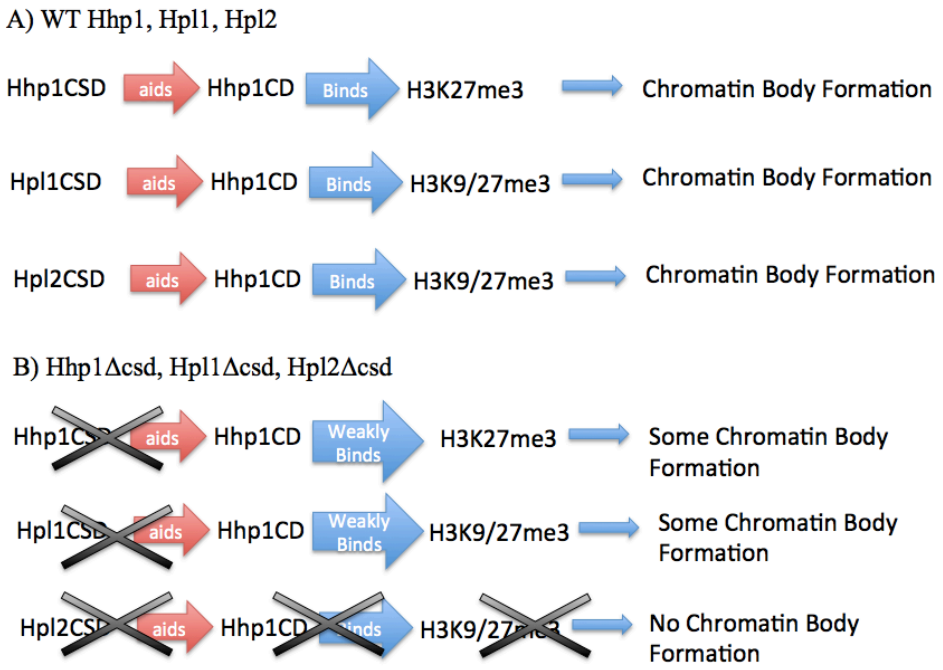

Figure 20. Proposed mechanism of the effect of the CSDs of Hhp1, Hpl1, and Hpl2 (Hhp1CSD, Hpl1CSD, Hpl2CSD) on chromatin body formation (A), and how the removal of the CSD could account for the results of this study (B).

The mechanism underlying the effect of the chromoshadow domains of Hhp1 and Hpl2 on the localization of the protein to chromatin bodies and therefore the potential effect on the chromodomains' affinity for H3K27me3 and H3K9me3 may involve the homodimerization of the CSD which affects the ability of the CSD to recruit PxVxL proteins (Grewal and Jia, 2007). This could mean that the differences in the effects of the CSD on localization to chromatin bodies is due to the influence of the homodimerization of the CSD on CD function. The homodimerization of the CSD of Hpl2 could be more critical to CD function than the homodimerization of the CSD of Hhp1 and Hpl1.

The difference in CSD function supported by these results also indicates a divergence of CSD functions in different proteins found in *T. thermophila.* Other CSD-containing proteins including Lia4, and Pdd1, may have similar mechanisms relating to

chromatin body formation. The dimerization of CSD of Lia4, another CSD-containing protein, may be required for the localization of Lia4 to IES, suggesting that the CSD of Lia4 has a similar function than that of Hpl2 (Horrell and Chalker, 2014). The dimerization of the CSD Pdd1, another HP1 like protein found in *T. thermophila* could recruit downstream excision and repair machinery (Schwope and Chalker, 2014). Pdd1 and Hpl1 and Hpl2 colocalize [data by Doug Chalker not shown] which could mean that these proteins interact to target IES sequences and eliminate them.

Implications for Human Health

The potential functions of CSD of Hpl1, Hpl2 and Hhp1 on the localization of these proteins to chromatin bodies and the potential mechanism underlying this could implicate human health. Human homologs of these proteins are involved in breast cancer and stem cells. The regulation of Heterochromatin protein $1^{Hs\alpha}$ correlates with the severity of breast cancer in humans (Norwood et al., 2006). Heterochromatin protein $1^{Hs\alpha}$ is down-regulated in breast cancer that is invasive and metastatic (Norwood et al., 2006). If this protein is expressed in very invasive cells, they become less invasive (Norwood et al., 2006). The ability to suppress invasion is caused by the ability of $HP1^{Hs\alpha}$ to dimerize, which involves the chromoshadow domain (Norwood et al., 2006). HP1β, another heterochromatin like protein in humans, is necessary for pluripotency in embryonic stem cells (Mattout et al, 2015). It is also needed for differentiated cells to differentiate properly (Mattout et al, 2015). Like the assumed function of the CSD of Hhp1, Hpl1 and Hpl2, the CSD of HP1β also homodimerizes to form a binding structure for PxVxL proteins (reviewed in Biller et al, 2010). The findings of this investigation of the CSD in

Hhp1, Hpl1 and Hpl2 may lead to more understanding of the effect of the CSD in HPL1β on the entire proteins function.

Limitations of Analysis

Ideally, the immmunoflourescence microscopy would allow for the colocalization of Hhp1Δcsd and Rhodamine stained H3K27me3 to determine if the histone modification was present in the anlagen but the protein did not localize to the histone modification which would suggest the CSD is needed for proper binding of H3K27me3. Additionally, the colocalization of chromatin bodies in Hhp1WT with H3K27me3 would confirm that the assay was accurate. However, the chromatin bodies were not well preserved when fixed in paraformaldehyde. When replicating this experiment, a higher concentration of paraformaldehyde is advised. Also, the rhodamine stain had a lot background, which decreased the clarity of the methyl marks. To improve this, the cells should be subjected to longer washes in PBST (a buffer) after exposure to primary and secondary antibody to increase the specificity of the antibodies.

Future Studies

In order to confirm that the difference in localization pattern seen in Hpl1Δcsd and Hpl2Δcsd were due to the CSD and not the lose of H3K27me3 or H3K9me3, the immunofluorescence stain with rhodamine and an antibody that targets H3K9me3 should be done. Colocalization of these stains with the GFP-tagged Hpl1Δcsd and Hpl2Δcsd could more conclusively suggest that the proteins were interacting with the methyl marks. Additionally, there were less mating pairs when Hpl2Δcsd was mated with B2. This

could mean that the CSD of Hpl2 may affect typical conjugation, which could be another phenomenon to investigate in detail. In addition, Hpl1Δcsd was found to localize to the basal bodies. Preliminary microscopy of Hpl1WT [data not shown] suggests that this localization to basal bodies may also occur. However, future investigations should be carried out to confirm this and to explore the function of CSD's in basal bodies.

To investigate CSD domain function more specifically, the CSD of Hhp1, Hpl1, and Hpl2 could be mutated at a region known to cause the homodimerization of the CSD. If the chromodomain deficient proteins localize to chromatin bodies, this would suggest that the dimerization of the CSD and subsequent binding of PxVxL proteins does not affect the localization of these proteins to chromatin bodies. Inserting a point mutation to disrupt homodimerization of the CSD would be ideal. This is because a point mutation will have less effect on protein folding than excising an entire region of the protein. The results found in this study could be due to dysfunctions due to misfolded proteins or a disruption in the ability of hinge region to be phosphorylated, which is associated with targeting of the protein to heterochromatin. Mutating only a certain region of the CSD may limit this disruption. The entire CSD was excised in this study instead of the point mutation because it was unknown if the entire CSD had an effect on protein localization.

Acknowledgements

I would like to thank Professor Wiley for her guidance and support with the lab work and with the written thesis and Professor Leconte for his corrections and editorial support with the written thesis. I would also like to thank Alyssa Yoshino for making the Hhp1Δcsd construct and Adrienne Hino, Chavi Checker, and Lizzie Kim for their assistance in the lab. I would like to awknowedge David Bagnani for his assistance with photoshop and Elizabeth Bagnani for her emotional support. Lastly, I thank the W. M. Keck Science Department for the lab space, lab materials and summer funding. This thesis is dedicated to my grandfather, Jerry Bagnani, who always encouraged me to excel in science.

References

Akai, Y., Adachi, N., Hayashi, Y., Eitoku, M., Sano, N., Natsume, R., Kudo, N., Tanokura, M., Senda, T., and Horikoshi, M. (2010). Structure of the histone chaperone CIA/ASF1-double bromodomain complex linking histone modifications and site-specific histone eviction. Proc. Natl. Acad. Sci. U.S.A. *107*, 8153–8158.

Badugu, R., Yoo, Y., Singh, P.B., and Kellum, R. (2004). Mutations in the heterochromatin protein 1 (HP1) hinge domain affect HP1 protein interactions and chromosomal distribution. Chromosoma *113*, 370–384.

Banerjee, T., and Chakravarti, D. (2011). A Peek into the Complex Realm of Histone Phosphorylation. Mol Cell Biol *31*, 4858–4873.

Bannister, A.J., Zegerman, P., Partridge, J.F., Miska, E.A., Thomas, J.O., Allshire, R.C., and Kouzarides, T. (2001). Selective recognition of methylated lysine 9 on histone H3 by the HP1 chromo domain. Nature *410*, 120–124.

Billur, M., Bartunik, H.D., and Singh, P.B. (2010). The essential function of HP1β: a case of the tail wagging the dog? Trends in Biochemical Sciences *35*, 115–123.

Boldrin, F., Santovito, G., Gaertig, J., Wloga, D., Cassidy-Hanley, D., Clark, T.G., and Piccinni, E. (2006). Metallothionein Gene from Tetrahymena thermophila with a Copper-Inducible-Repressible Promoter. Eukaryot Cell *5*, 422–425.

Bowman, G.D., and Poirier, M.G. (2015). Post-translational modifications of histones that influence nucleosome dynamics. Chem. Rev. *115*, 2274–2295.

Burgess, R.J., Zhou, H., Han, J., and Zhang, Z. (2010). A role for Gcn5 in replication-coupled nucleosome assembly. Mol. Cell *37*, 469–480.

Campos, E.I., and Reinberg, D. (2009). Histones: annotating chromatin. Annu. Rev. Genet. *43*, 559–599.

Cheung, P., Allis, C.D., and Sassone-Corsi, P. (2000). Signaling to Chromatin through Histone Modifications. Cell *103*, 263–271.

Collins, K., and Gorovsky, M.A. (2005). Tetrahymena thermophila. Current Biology *15*, R317–R318.

Di Cerbo, V., Mohn, F., Ryan, D.P., Montellier, E., Kacem, S., Tropberger, P., Kallis, E., Holzner, M., Hoerner, L., Feldmann, A., et al. (2014). Acetylation of histone H3 at lysine 64 regulates nucleosome dynamics and facilitates transcription. eLife *3*.

Di Croce, L., and Shiekhattar, R. (2008). Thrilling transcription through threonine phosphorylation. Nat. Cell Biol. *10*, 5–6.

Eissenberg, J.C., and Elgin, S.C.R. (2014). HP1a: a structural chromosomal protein regulating transcription. Trends Genet. *30*, 103–110.

Eissenberg, J.C., Ge, Y.W., and Hartnett, T. (1994). Increased phosphorylation of HP1, a heterochromatin-associated protein of Drosophila, is correlated with heterochromatin assembly. J. Biol. Chem. *269*, 21315–21321.

Fischle, W., Tseng, B.S., Dormann, H.L., Ueberheide, B.M., Garcia, B.A., Gorovsky, M.A. (1980). Genome Organization and Reorganization in Tetrahymena. Annual Review of Genetics *14*, 203–239.

Grewal, S.I.S., and Jia, S. (2007). Heterochromatin revisited. Nat. Rev. Genet. *8*, 35–46.

Han, Y., and Garcia, B.A. (2013). Combining genomic and proteomic approaches for epigenetics research. Epigenomics *5*, 439–452.
Hatanaka, Y., Inoue, K., Oikawa, M., Kamimura, S., Ogonuki, N., Kodama, E.N., Ohkawa, Y., Tsukada, Y., and Ogura, A. (2015). Histone chaperone CAF-1 mediates repressive histone modifications to protect preimplantation mouse embryos from endogenous retrotransposons. Proc. Natl. Acad. Sci. U.S.A. *112*, 14641–14646.
Hayashi, Y., Senda, T., Sano, N., and Horikoshi, M. (2009). Theoretical framework for the histone modification network: modifications in the unstructured histone tails form a robust scale-free network. Genes Cells *14*, 789–806.
Hergeth, S.P., and Schneider, R. (2015). The H1 linker histones: multifunctional proteins beyond the nucleosomal core particle. EMBO Reports *16*, 1439–1453.
Herrmann, H., and Zwerger, M. (2010). The danger of "multi-tasking": LBR out of control. Nucleus *1*, 319–324.
Hendzel, M.J., Wei, Y., Mancini, M.A., Van Hooser, A., Ranalli, T., Brinkley, B.R., Bazett-Jones, D.P., and Allis, C.D. (1997). Mitosis-specific phosphorylation of histone H3 initiates primarily within pericentromeric heterochromatin during G2 and spreads in an ordered fashion coincident with mitotic chromosome condensation. Chromosoma *106*, 348–360.
Horrell, S.A., and Chalker, D.L. (2014). LIA4 Encodes a Chromoshadow Domain Protein Required for Genomewide DNA Rearrangements in Tetrahymena thermophila. Eukaryot Cell *13*, 1300–1311.
Hsu, J.-Y., Sun, Z.-W., Li, X., Reuben, M., Tatchell, K., Bishop, D.K., Grushcow, J.M., Brame, C.J., Caldwell, J.A., Hunt, D.F., et al. (2000). Mitotic Phosphorylation of Histone H3 Is Governed by Ipl1/aurora Kinase and Glc7/PP1 Phosphatase in Budding Yeast and Nematodes. Cell *102*, 279– 291.
Huang, H., Wiley, E.A., Lending, C.R., and Allis, C.D. (1998). An HP1-like protein is missing from transcriptionally silent micronuclei of Tetrahymena. Proc. Natl. Acad. Sci. U.S.A. *95*, 13624–13629.
Huang, H., Smothers, J.F., Wiley, E.A., and Allis, C.D. (1999). A nonessential HP1-like protein affects starvation-induced assembly of condensed chromatin and gene expression in macronuclei of Tetrahymena thermophila. Mol. Cell. Biol. *19*, 3624–3634.
Jamieson, K., Wiles, E.T., McNaught, K.J., Sidoli, S., Leggett, N., Shao, Y., Garcia, B.A., and Selker, E.U. (2016). Loss of HP1 causes depletion of H3K27me3 from facultative heterochromatin and gain of H3K27me2 at constitutive heterochromatin. Genome Res *26*, 97–107.
Jenuwein, T., and Allis, C.D. (2001). Translating the Histone Code. Science *293*, 1074–1080.
Kouzarides, T. (2007). Chromatin modifications and their function. Cell *128*, 693–705.
Lachner, M., O'Carroll, D., Rea, S., Mechtler, K., and Jenuwein, T. (2001). Methylation of histone H3 lysine 9 creates a binding site for HP1 proteins. Nature *410*, 116–120.
Laughlin, M.H., Padilla, J., Jenkins, N.T., Thorne, P.K., Martin, J.S., Rector, R.S., Akter, S., and Davis, J.W. (2015). Exercise-induced differential changes in gene

expression among arterioles of skeletal muscles of obese rats. J. Appl. Physiol. *119*, 583–603.
Law, M.J., and Ciccaglione, K. (2015). Fine-Tuning of Histone H3 Lys4 Methylation During Pseudohyphal Differentiation by the CDK Submodule of RNA Polymerase II. Genetics *199*, 435–453.
Lechner, M.S., Begg, G.E., Speicher, D.W., and Rauscher, F.J. (2000). Molecular Determinants for Targeting Heterochromatin Protein 1-Mediated Gene Silencing: Direct Chromoshadow Domain–KAP-1 Corepressor Interaction Is Essential. Mol. Cell. Biol. *20*, 6449–6465.
Lechner, M.S., Schultz, D.C., Negorev, D., Maul, G.G., and Rauscher, F.J. (2005). The mammalian heterochromatin protein 1 binds diverse nuclear proteins through a common motif that targets the chromoshadow domain. Biochem. Biophys. Res. Commun. *331*, 929–937.
Lin, C.-H., Li, B., Swanson, S., Zhang, Y., Florens, L., Washburn, M.P., Abmayr, S.M., and Workman, J.L. (2008). Heterochromatin protein 1a stimulates histone H3 lysine 36 demethylation by the Drosophila KDM4A demethylase. Mol. Cell *32*, 696–706.
Liu, Y., Mochizuki, K., and Gorovsky, M.A. (2004). Histone H3 lysine 9 methylation is required for DNAelimination in developing macronuclei in Tetrahymena. Proc. Natl. Acad. Sci. U.S.A. *101*, 1679–1684.
Lomberk, G., Wallrath, L., and Urrutia, R. (2006). The Heterochromatin Protein 1 family. Genome Biol. *7*, 228.
Luger, K., Mäder, A.W., Richmond, R.K., Sargent, D.F., and Richmond, T.J. (1997). Crystal structure of the nucleosome core particle at 2.8 Å resolution. Nature *389*, 251–260.
Mattout, A., Aaronson, Y., Sailaja, B.S., Raghu Ram, E.V., Harikumar, A., Mallm, J.-P., Sim, K.H., Nissim-Rafinia, M., Supper, E., Prim B. Singh, et al. (2015). Heterochromatin Protein 1β (HP1β) has distinct functions and distinct nuclear distribution in pluripotent versus differentiated cells. Genome Biology *16*, 213.
Mishima, Y., Watanabe, M., Kawakami, T., Jayasinghe, C.D., Otani, J., Kikugawa, Y., Shirakawa, M., Kimura, H., Nishimura, O., Aimoto, S., et al. (2013). Hinge and Chromoshadow of HP1α Participate in Recognition of K9 Methylated Histone H3 in Nucleosomes. Journal of Molecular Biology *425*, 54–70.
Miao, W., Xiong, J., Bowen, J., Wang, W., Liu, Y., Braguinets, O., Grigull, J., Pearlman, R.E., Orias, E., and Gorovsky, M.A. (2009). Microarray Analyses of Gene Expression during the Tetrahymena thermophila Life Cycle. PLOS ONE *4*, e4429.
Nakayama, J., Rice, J.C., Strahl, B.D., Allis, C.D., and Grewal, S.I.S. (2001). Role of Histone H3 Lysine 9 Methylation in Epigenetic Control of Heterochromatin Assembly. Science *292*, 110–113.
Norwood, L.E., Moss, T.J., Margaryan, N.V., Cook, S.L., Wright, L., Seftor, E.A., Hendrix, M.J.C., Kirschmann, D.A., and Wallrath, L.L. (2006). A requirement for dimerization of HP1Hsalpha in suppression of breast cancer invasion. J. Biol. Chem. *281*, 18668–18676.
Richart, A.N., Brunner, C.I.W., Stott, K., Murzina, N.V., and Thomas, J.O. (2012). Characterization of Chromoshadow Domain-mediated Binding of

Heterochromatin Protein 1 (HP1) to Histone H3. Journal of Biological Chemistry *287*, 18730–18737.
Rothbart, S.B., and Strahl, B.D. (2014). Interpreting the language of histone and DNA modifications. Biochim. Biophys. Acta *1839*, 627–643.
San-Segundo, P.A., and Roeder, G.S. (2000). Role for the silencing protein Dot1 in meiotic checkpoint control. Mol. Biol. Cell *11*, 3601–3615.
Santos-Rosa, H., Schneider, R., Bannister, A.J., Sherriff, J., Bernstein, B.E., Emre, N.C.T., Schreiber, S.L., Mellor, J., and Kouzarides, T. (2002). Active genes are t tri-methylated at K4 of histone H3. Nature *419*, 407–411.
Schwope, R.M., and Chalker, D.L. (2014). Mutations in Pdd1 reveal distinct requirements for its chromodomain and chromoshadow domain in directing histone methylation and heterochromatin elimination. Eukaryotic Cell *13*, 190–201.
Schwartzman, O., and Tanay, A. (2015). Single-cell epigenomics: techniques and emerging applications. Nat Rev Genet *16*, 716–726.
Seeler, J.-S., Marchio, A., Sitterlin, D., Transy, C., and Dejean, A. (1998). Interaction of SP100 with HP1 proteins: A link between the promyelocytic leukemia-associated nuclear bodies and the chromatin compartment. PNAS *95*, 7316–7321.
Shogren-Knaak, M., Ishii, H., Sun, J.-M., Pazin, M.J., Davie, J.R., and Peterson, C.L. (2006). Histone H4-K16 acetylation controls chromatin structure and protein interactions. Science *311*, 844–847.
Suganuma, T., and Workman, J.L. (2011). Signals and combinatorial functions of histone modifications. Annu. Rev. Biochem. *80*, 473–499.
Suka, N., Suka, Y., Carmen, A.A., Wu, J., and Grunstein, M. (2001). Highly specific antibodies determine histone acetylation site usage in yeast heterochromatin and euchromatin. Mol. Cell *8*, 473–479.
Taunton, J., Hassig, C.A., and Schreiber, S.L. (1996). A mammalian histone deacetylase r related to the yeast transcriptional regulator Rpd3p. Science *272*, 408–411.
Thiru, A., Nietlispach, D., Mott, H.R., Okuwaki, M., Lyon, D., Nielsen, P.R., Hirshberg, M., Verreault, A., Murzina, N.V., and Laue, E.D. (2004). Structural basis of HP1/PXVXL motif peptide interactions and HP1 localisation to heterochromatin. EMBO J. *23*, 489–499.
Trojer, P., and Reinberg, D. (2007). Facultative heterochromatin: is there a distinctive molecular signature? Mol. Cell *28*, 1–13.
Villegas-Ruiz, V., Moreno, J., Jacome-Lopez, K., Zentella-Dehesa, A., and Juarez-Mendez, S. (2016). Quality Control Usage in High-Density Microarrays Reveals Differential Gene Expression Profiles in Ovarian Cancer. Asian Pac. J. Cancer Prev. *17*, 2519–2525.
Wagner, E.J., and Carpenter, P.B. (2012). Understanding the language of Lys36 methylation at histone H3. Nat. Rev. Mol. Cell Biol. *13*, 115–126.
Walter, D., Matter, A., and Fahrenkrog, B. (2014). Loss of histone H3 methylation at lysine 4 triggers apoptosis in Saccharomyces cerevisiae. PLoS Genet. *10*, e1004095.
Wang, J., Jia, S.T., and Jia, S. (2016). New Insights into the Regulation of Heterochromatin. Trends in Genetics *32*, 284–294.
Xu, J., Yuan, Y., Liang, A., and Wang, W. (2015). Chromodomain protein Tcd1 is

required for macronuclear genome rearrangement and repair in Tetrahymena. Sci Rep *5*, 10243.
Yale, K., Tackett, A.J., Neuman, M., Bulley, E., Chait, B.T., and Wiley, E. (2016). Phosphorylation-Dependent Targeting of Tetrahymena HP1 to Condensed Chromatin. mSphere *1*, e00142–16.
Yao, M.-C., Chao, J.-L., and Cheng, C.-Y. (2014). Programmed Genome Rearrangements in Tetrahymena. Microbiol Spectr *2*.
Zhao, T., and Eissenberg, J.C. (1999). Phosphorylation of Heterochromatin Protein 1 by Casein Kinase II Is Required for Efficient Heterochromatin Binding inDrosophila. J. Biol. Chem. *274*, 15095–15100.